Conceptual Model Update of the Sorik Marapi Geothermal Prospect, Sumatra, Indonesia

Nicholas Hinz[1], Gabe Matson[1], David Sussman[1], Jill Haizlip[1], Jesse Turk[1], Colin Carver[1], Steven Fercho[4], Ridha Hendri[3], Haris Siagian[3], Amanda Fishbin[1], William Cumming[2], Amelia Letvin[1], Alex Milton[1]

[1]Geologica Geothermal Group, Inc., 5 Third Street Suite 420, San Francisco, CA 94103

[2]Cumming Geoscience, 4728 Shade Tree Lane, Santa Rosa CA 95405

[3]PT Sorik Marapi Geothermal Power, Recapital Building 5th Floor, Jl Adityawarman Kav 55, Jakarta Selatan 12160

[4]Fervo Energy (formerly with Geologica)

nhinz@geologica.net

Keywords

Structural geology, volcano-hosted geothermal system, Sumatran fault, strike-slip fault, conceptual model, geologic model

ABSTRACT

At the Sorik Marapi Geothermal Power (SMGP) field in North Sumatra, 32 deep wells have proven a ~245 to 325°C geothermal resource extending over an area greater than 2.5 km (E-W) x 3 km (N-S) along a main segment of the Sumatran Fault System (SFS) about 4 km northeast of Sorik Marapi volcano. This conceptual model update incorporates new well data including new and revised temperature and pressure logs, production test results and borehole geology extensively revised based on thin section analysis. Important new surface data includes surface geology and LiDAR structure analyses as well as an expanded MT survey and 3D inversion. Previous published conceptual models of the Sorik Marapi resource have fallen into two main groups: (1) a >300°C upflow centered under the magmatic volcanic edifice that then outflows to the northeast and neutralizes as it reaches the wellfield, and (2) a separate >300°C neutral upflow along the SFS NE of the volcano. In the revised conceptual model presented here, the vapor core of Sorik Marapi is isolated to a chimney underlying the volcano's summit area and the geothermal reservoir is a hydrologically separate, neutral >320°C upflow about 1 km west of the main strand of the active SFS, with associated elongate <260°C outflows to the north and south. The revised stratigraphy, alteration, structural model, and subsurface temperature pattern show that the reservoir permeability is controlled by complex subsidiary faults interacting with formation properties, primary permeability and hydrothermal alteration. New image logs collected from three wells indicate a wide range of open fracture orientations and those associated with major feed zones do not correspond to surface fault traces, although the mapped active Quaternary faults define the overall geometry of the reservoir. Unlike other geothermal systems that have been impacted by magmatic acid vapor cores or supergene acid influx, there is

no evidence that the Sorik Marapi geothermal reservoir has experienced either, rather the reservoir is geochemically similar to many other entirely neutral systems developed worldwide.

1. Introduction

The Sorik Marapi geothermal field (Sorik Marapi) is located on the lower northeast flank of Sorik Marapi volcano and along a major active strand of the Sumatra Fault System in North Sumatra (Figure 1). Sorik Marapi was initially studied by industry and academia in the 1980s and 1990s (e.g., Hochstein and Sudarman, 1993). The first comprehensive geothermal assessment of Sorik Marapi was completed by Sinclair Knight Merz (SKM) in 2011, and involved geology, geochemistry, and geophysics studies, in addition to drilling three shallow slim wells (SKM, 2011). This assessment by SKM (2011) concluded that up to 4 possible resource areas were present along discrete parts of the SFS NE of the Sorik Marapi volcanic edifice (Figure 2). Sorik Marapi Geothermal Power (SMGP) has drilled >30 wells (Figure 3) since 2016 and has proven a ~245° to 325°C geothermal resource extending over an area greater than 2.5 x 3 km in Sibanggor, the southernmost of the four prospect areas identified by SKM (2011).

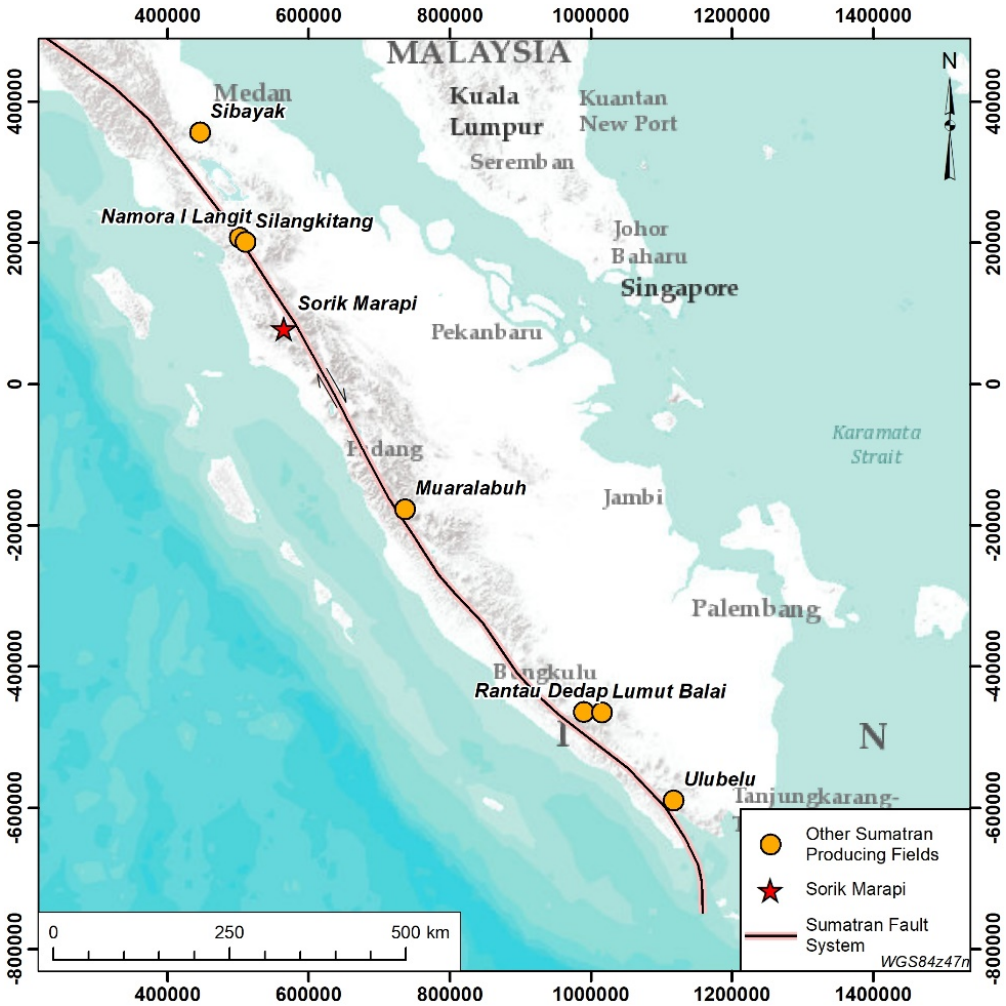

Figure 1. Location map of the Sorik Marapi geothermal prospect in the context of producing geothermal fields on Sumatra, Indonesia and the Sumatran fault system.

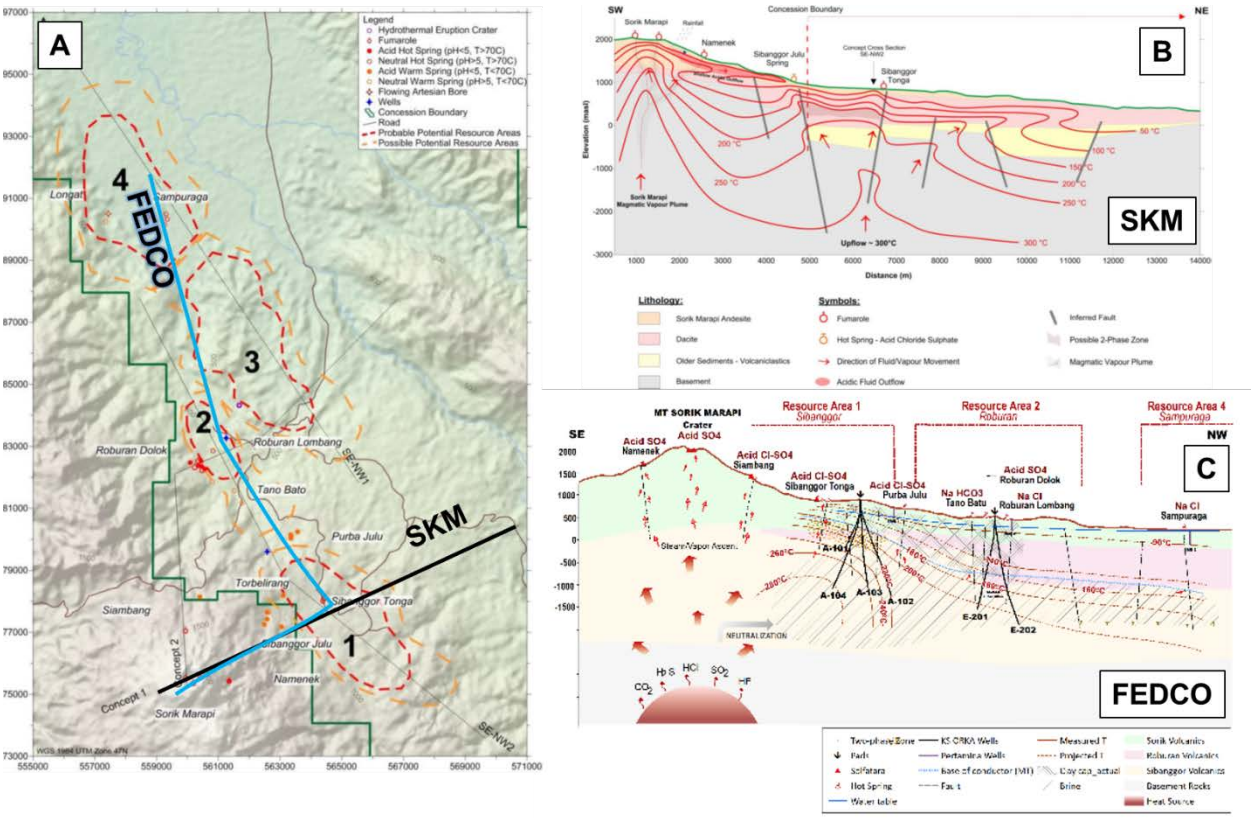

Figure 2. (a) Sorik Marapi conceptual model map from SKM (2011). Resource area numbers and names referred to in this paper: 1) Sibanggor, 2) Roburan, 3) South Sampuraga, 4) North Sampuraga. (b) Cross sections through SKM (2011) and (c) Fedco (Licup et al., 2017) conceptual models.

1. Exploration History

In 2011 SKM conducted geologic, geochemical, and geophysical studies of Sorik Marapi and concluded that there may be up to four separate resource areas/geothermal systems, numbered and named from south to north: 1) Sibanggor, 2) Roburan, 3) South Sampuraga, and 4) North Sampuraga (Figure 2). The extent of each resource area was strongly influenced by the MT and outline of the conductor(s), although geology, geochemistry, and other geophysics (gravity) also played a role. SKM (2011) concluded that the Sibanggor resource was the lowest risk area to target for exploration drilling and possible development. The pre-drilling model of the Sibanggor reservoir was based on the location and geometry of the MT conductor and fumaroles with promising geochemistry. SKM (ibid) proposed that a geothermal reservoir was likely hosted partly in volcanics and partly in pre-Tertiary basement rock, the permeability for which would likely be controlled by fractures and faulting associated with the SFS. The expected reservoir rock and permeability pattern proposed by SKM were consistent with a conceptual model in which the Sibanggor resource is associated with upflow along part of the SFS rather than under the center of the volcanic edifice.

Starting in 2016 and extending into mid-2021 (time of writing this paper), SMGP has drilled 32 wells (Figure 3) to depths of 1500 to 2650 m and distributed across parts of the southern two possible resource areas identified by SKM (2011). Most of the wells have been drilled in the Sibanggor area, which is the southernmost area in the SKM assessment, and these have proven a

~245° to 325°C geothermal resource extending over an area greater than 2.5 km (E-W) x 3 km (N-S) along a main segment of the SFS about 4 km northeast of Sorik Marapi volcano (Figure 2).

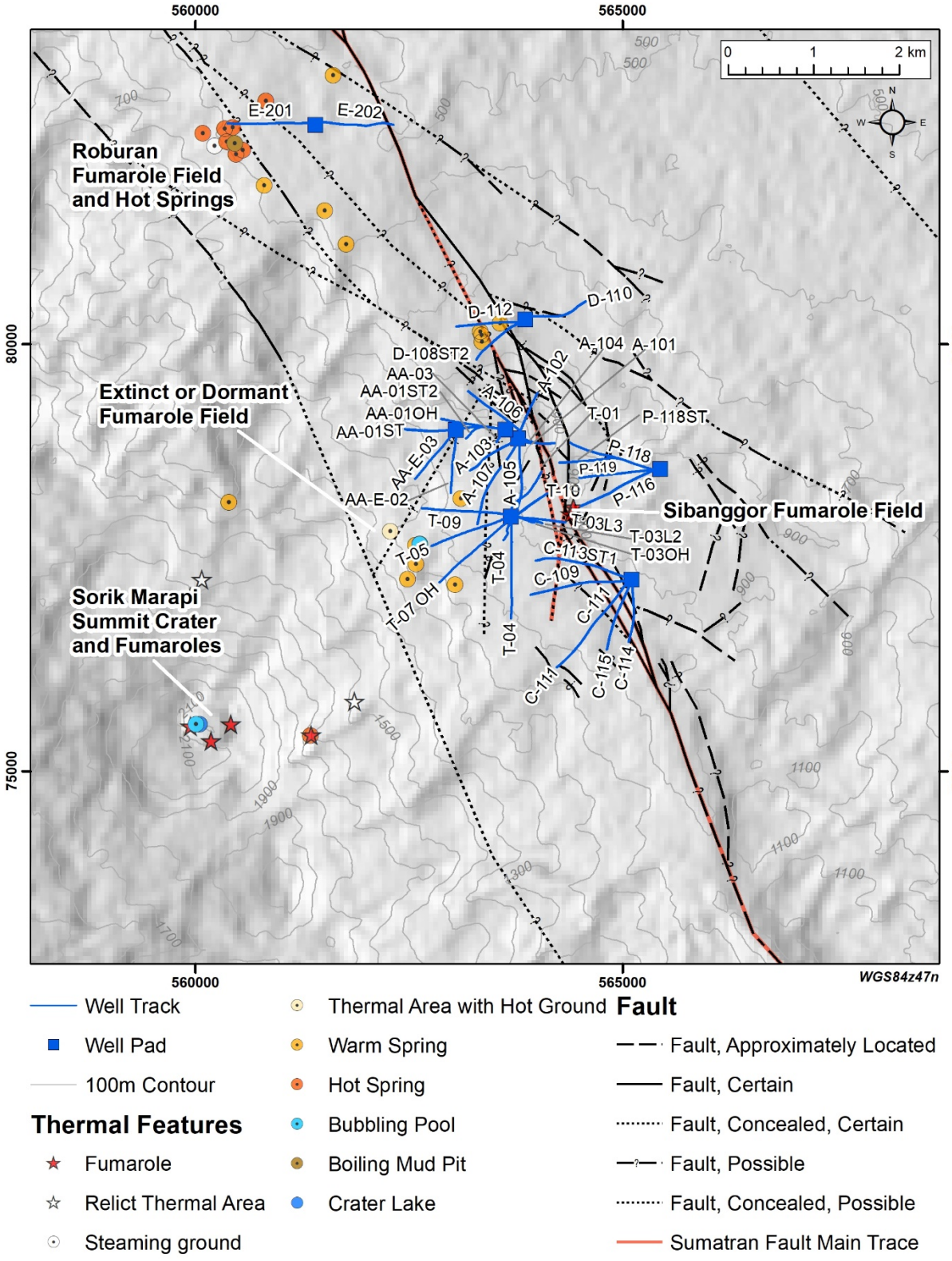

Figure 3: Modern well field at Sorik Marapi including surface manifestations and updated fault mapping.

Based on initial drilling results by SMPG, Sarmiento et al. (2017) and Licup et al. (2017) presented an alternative model to the original by SKM, positing an upflow beneath the summit of Sorik Marapi volcano that outflowed to the NE, where the reservoir fluids were neutralized after circulating through a thick sequence of volcanic rocks (Figure 2). This alternative model was also built around a stratigraphic model in which the resource was associated with three volcanic rock sequences rather than potentially including pre-volcanic basement rock as had been proposed in the SKM model.

2. Data used in the conceptual model update

This conceptual model update reflects new information derived from the drilling and testing of 10 new wells, and includes fluid and non-condensable gas geochemistry, static and dynamic temperature and pressure surveys, well lithologies and hydrothermal alteration, and tracer studies. The Phase 1 power plants (45 MW) have been operating since December 2019, and the Phase 2 power plants (45 MW) are currently nearing completion. All of the wells for Phases 1 and 2 have been completed, while drilling for a third phase (50 MW), which is expected to be on-line in early 2022, is currently underway. This conceptual model update builds on the earlier model of Carver and Hidayat (2020) and provides an update on well temperature and flowtest data, geochemistry, lithology and alteration from thin section petrography, and geophysical modeling.

2.1 Geology

A major update to the stratigraphic framework was completed in late 2019 and early 2020. This involved reanalyzing cuttings from the first 19 wells under a binocular microscope, analyzing thin sections of cuttings from these wells, and integrating these data with lithologic data from the new Pad T, P, AA, and AA-EXT wells. Previously, the lithologic units were grouped into three volcanic formations across Pads A, C, D, E, and P, named (from youngest to oldest): Sorik, Roburan, and Sibanggor (Figure 2, Licup et al., 2017). Updated lithologic logs were based on integrating observations from both binocular microscope analysis and petrographic analysis (Figure 4), which resulted in the identification of several new lithologies that were grouped into the following five formations: 1) Quaternary Intrusions, 2) Quaternary-Tertiary Volcanics, 3) Tertiary Sediments, 4) Mesozoic or Paleozoic granite, and 5) Mesozoic or Paleozoic metasediments.

The oldest formations comprise Paleozoic and/or Mesozoic metasediments, which include phyllite, schist, quartzite, slate, and carbonates, and are present in Pad T, C, A, AA, and AA-Ext wells. Similar metamorphic units are exposed 3.3 km WNW of Pad A in both deposition and fault contact with overlying QTv (Figure 5). The metasediments are intruded by Paleozoic and/or Mesozoic granite (gr) that are present in C-115, C-114, T-02, and possibly T-04. Similar granites are also exposed about 10 km to the west, southeast, and northeast from the Pad A-T-C area (Figure 4). Miocene(?) clastic sediments (Ts) rest on the metamorphic rocks and granite and consist of medium to course-grained sandstone and pebble conglomerates with clasts eroded from underlying basement units. These Miocene sediments are encountered in Pad P wells, E-202, and all Pad D wells, and correlative rocks are exposed 6-7 km east of the reservoir (Figure 5). Based on well data, the Miocene sediments range up to more than 1800 m thick. Quaternary

to Tertiary age volcanics (QTv), consisting of interlayered felsic to intermediate composition lavas and tuffs rest on the Miocene sediments and volcanics, and older metamorphic rocks. The Qtv is present in all wells and reaches >2 km in thickness. The youngest unit is group of felsic porphyry intrusive rocks (QTi) that is intersected by Pad A wells and T-01. These rocks intrude the metasediments and the base of the Quaternary-Tertiary volcanic section, and reach ~700 m thick based on well data. All Pad A wells that intersect these intrusive rocks encountered total loss of circulation (TLC) during drilling, and absent a few core samples taken below TLC, there are no cuttings returns to confirm what lithologies are present at greater depths in these wells. Of these formations, reservoir production is mostly hosted in the metasediments and the Quaternary intrusive rocks, with only minor production from the granite and the Quaternary-Tertiary volcanics (feed zones noted in Figure 4).

Detailed geologic mapping has not been conducted at Sorik Marapi. The map in Figure 5 was compiled from Rock et al. (1983) and modified by reanalysis of LiDAR data by Geologica in 2018 and 2019, brief reconnaissance mapping by Geologica in 2019, new detailed well lithologic logs compiled in 2019 and 2020, and new geologic cross-sections linking map and well data, and modeling in Leapfrog to map out the structure and stratigraphy in 3D. The resulting map constitutes the most up-to-date map of the resource area. In 2019 Geologica and SMGP completed some mapping of the outcrop of metasediments exposed WNW of Pad A (MPu, Figure 4). This exposure of metasediments had not previously been placed on a map and is key to locally defining the location of one of the major western strands of the SFS, which may also bound the western side of the reservoir. The new 2020 well logs informed key updates to the map, in particular defining major strands of the Sumatran fault zone based on stratigraphic offsets based on the well data.

Analysis of well temperature and alteration mineralogy data has identified that the alteration of the cap overlying the reservoir varies from argillic to mixed clay to phyllic-propylitic. The cap geometry over major feed zones in production wells on Pads A, AA, AA-EXT and T in the north and wells C-113ST and C-109 in the south shows that reservoir top deepens to the southwest from Pad A and is deepest in the T-05 and T-09 area. Below the cap, the top of the reservoir in the Pad A wells area varies 300 m vertically from +260 masl to -50 masl, with consistent deepening to the southwest. In general, decreases in MeB values provide the most consistent marker for the top of the reservoir in this area, coupled with the appearance of chlorite replacement of phenocrysts; this is typical of the argillic to transitional/mixed clay transition. As the cap further deepens to the SW in the west-directed Pad T wells (i.e., T-05, T-07 and T-09), the cap to the reservoir is characterized by phyllic-propylitic alteration, and the underlying reservoir most consistently marked by the appearance of wairakite.

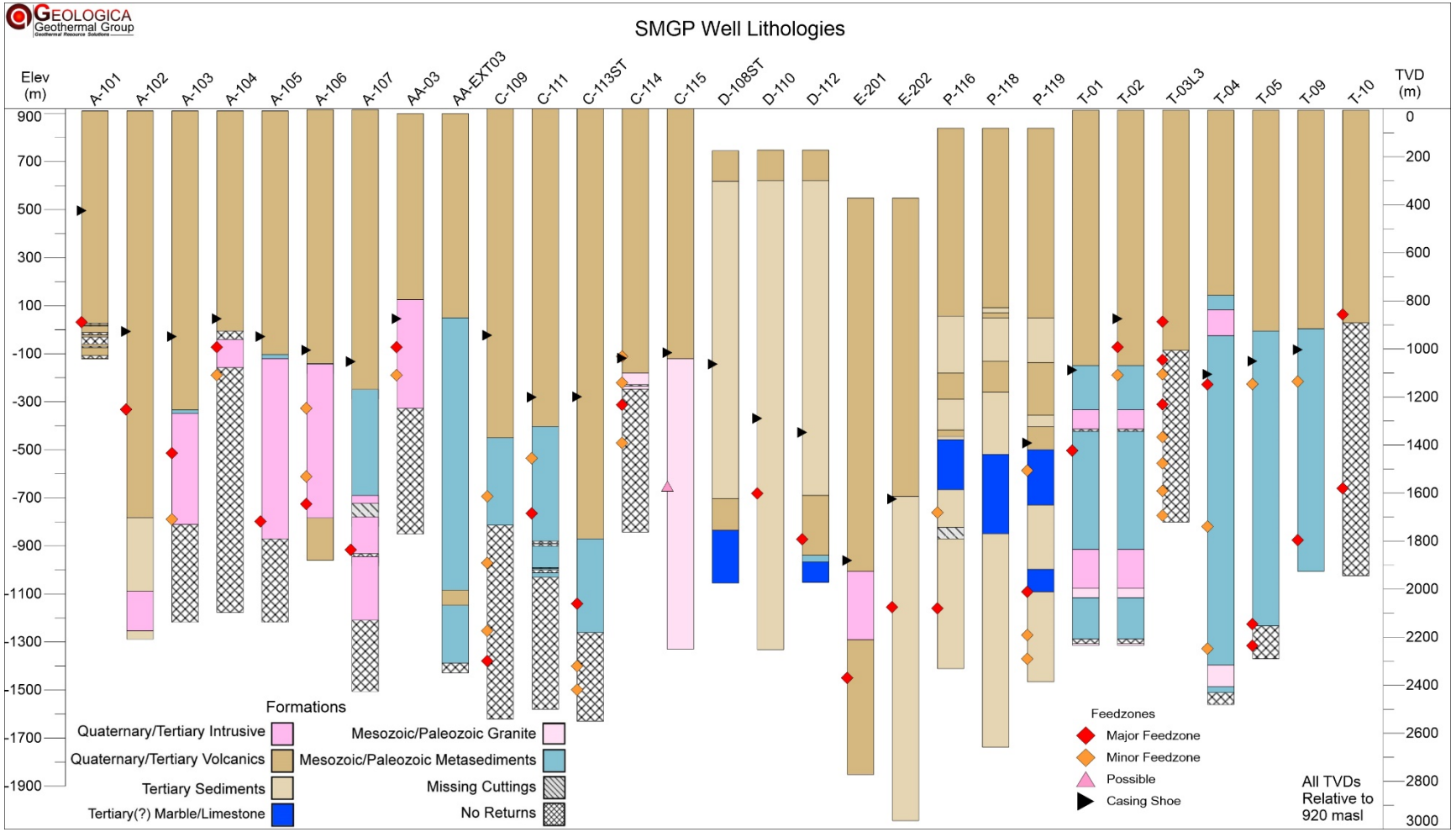

Figure 4. Well stratigraphy summary logs with casing points and feed zone distributions.

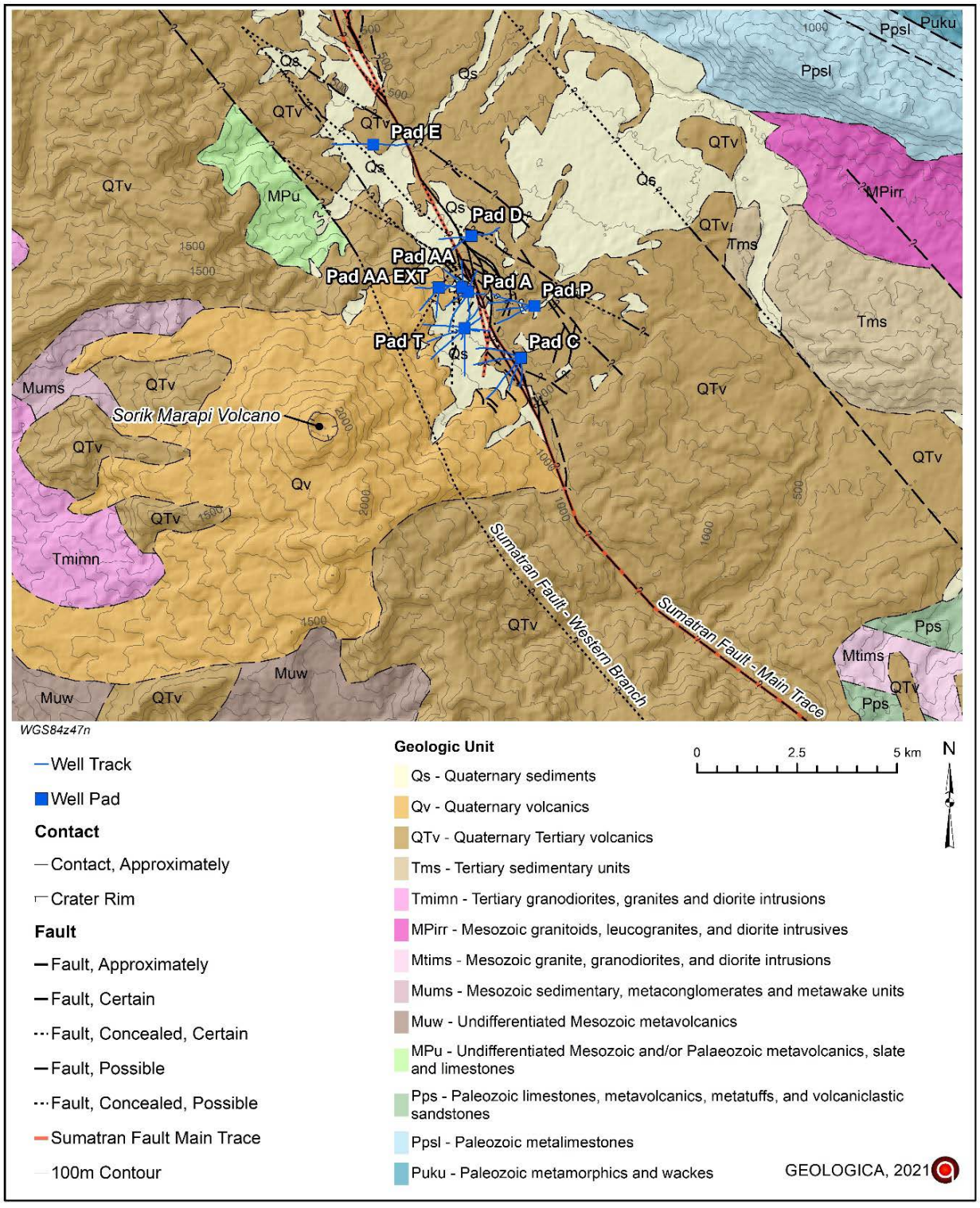

Figure 5. Updated geologic map of the region based on integrating field observations in 2018 - 2019, new drilling data, and original 1:250,000 scale mapping by Rock et al., (1983).

2.2 Geochemistry

Two-phase samples have been collected from 12 wells located on Pad A, C, and T, all located within the Sibanggor region. Two-phase samples of steam and brine were corrected to reservoir conditions assuming iso-enthalpic boiling from liquid at measured major feedzone temperature in each well and the saturated sampling conditions. Geochemical data from all wells indicates the Sorik Marapi reservoir is composed of dilute (TDS ~1500-1900 mg/kg) neutral Na-Cl brine. The reservoir non-condensable gas (NCG) is low concentration (up to 0.1 wt% total NCG) and primarily composed of CO_2, with minor portions of H_2S and trace amounts of NH_3, N_2, CH_4, and H_2.

Silica geothermometry of wells indicates reservoir temperatures of 240-290°C, with the highest silica geothermometer and measured temperatures is western Pad A and Pad T wells: A-103, A-107, T-05, and T-09. Na/K cation geothermometer applied to all wells are approximately 10 to 30°C higher than silica and measured temperatures, and indicate a maximum reservoir temperature of ~300°C. The highest measured temperatures in the field are in static surveys of wells T-07 and T-09 collected after well discharge testing (319°C and 324°C, respectively), which are considerably higher than both the silica geothermometers in those wells and the cation geothermometers of all wells. This supports that there is conductive heat input with higher temperatures than the convective heat input.

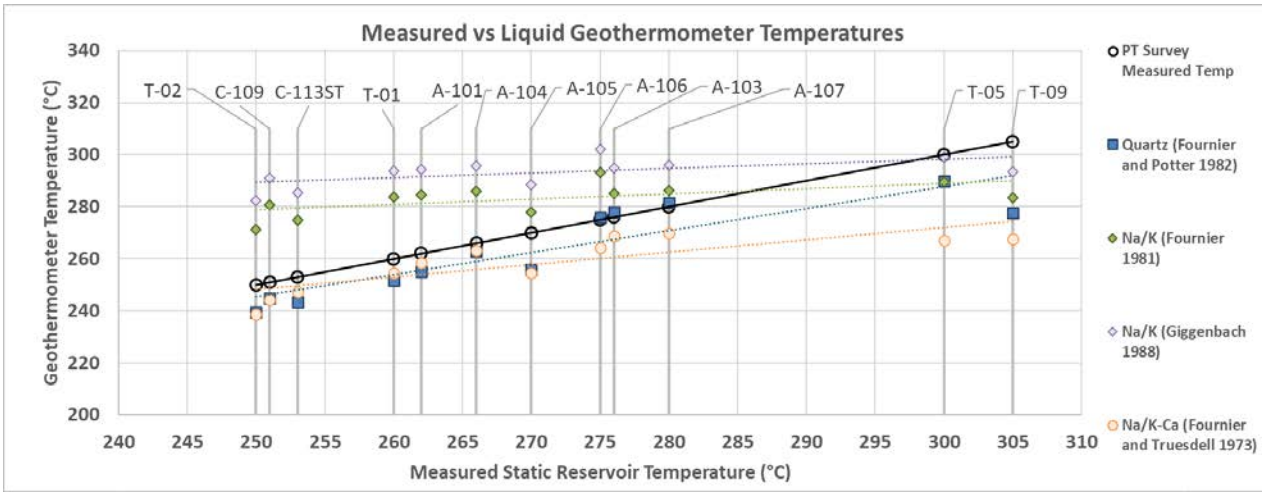

Figure 6. Liquid geothermometers and measured temperatures are plotted against each other for each well. Measured temperatures are based on downhole surveys collected near the time of geochemical sampling, some wells (A-105, A-107, T-05, T-09) have heated up considerably in since geochemical sampling.

2.3 Geophysics

Magnetotelluric (MT) resistivity imaging resolves several key conceptual model components. PT Sorik Marapi Geothermal Power commissioned two, wide-spread MT surveys with average station spacing from 600-800m (Figure 7). The 2011 survey conducted by WesternGeco, focused

on areas along the SFS from the Sibanggor fumarole fields to north of the Sampuraga surface manifestations (200 stations). The 2018 survey (108 stations) conducted by PT TBU targeted the summit and flanks of the Sorik Marapi volcano.

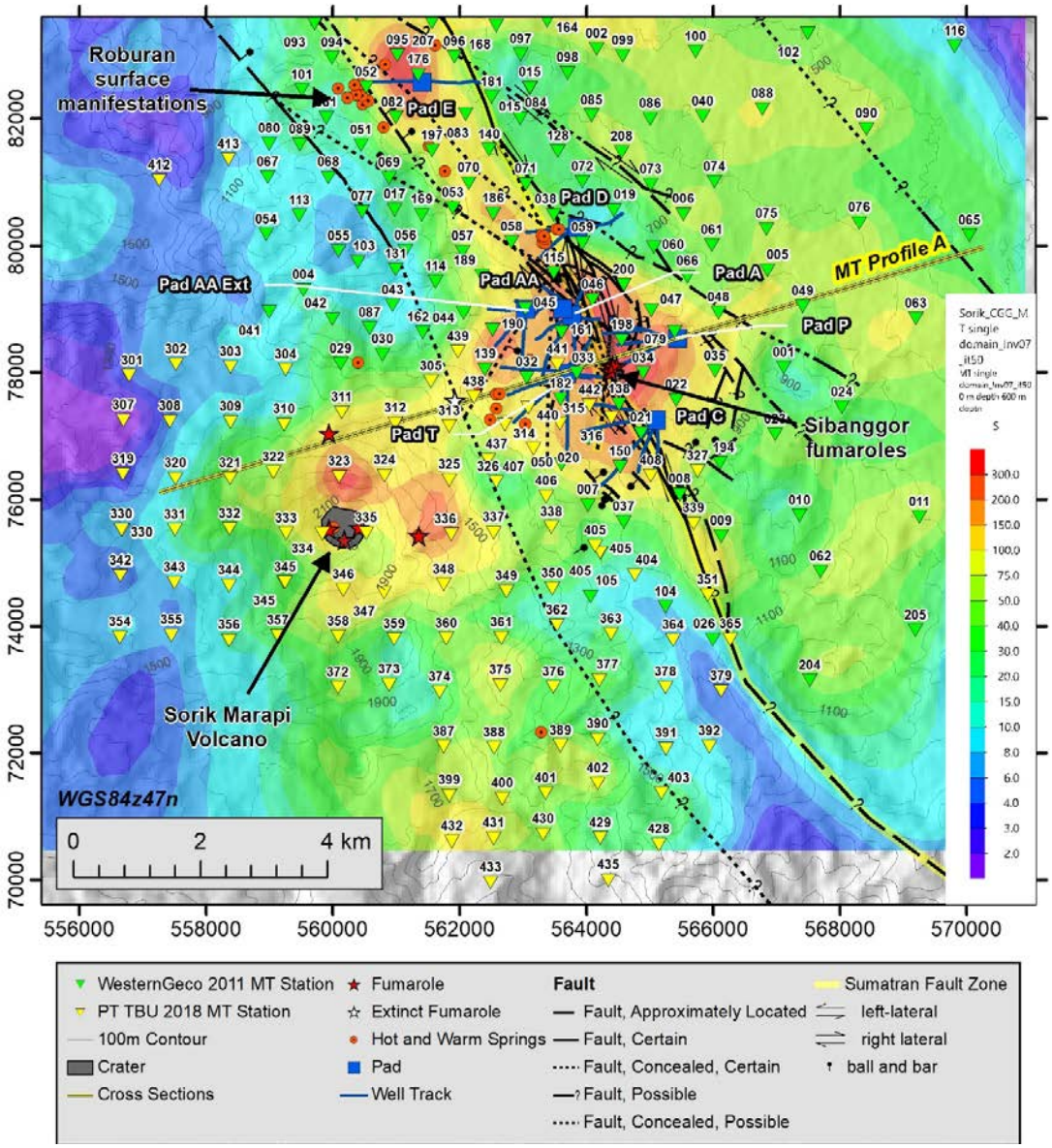

Figure 7: Map of 3D cumulative conductance from surface to 600m depth.

Matson et al. (2021) interpreted the MT resistivity models in context with our resource conceptual model. The key features resolved by MT include low resistivity argillic alteration associated with the neutral geothermal resource, low resistivity altered clays associated with the Sorik Marapi volcano magma core, moderate resistivity unaltered QTv and Ts east of the SFS, and possible gently shallowing low resistivity cap suggesting distal outflow to the north (Matson et al., 2021). The locus of the low resistivity zone (1.5 – 3 Ωm) is located around the Sibanggor Julu fumarole field and well Pads A, T, and C. The low resistivity zone is interpreted as argillic

alteration clays associated with shallow boiling near the top of the water table beneath the fumaroles. The low resistivity zone encompasses an area ~2.5km wide in the WSW-ENE direction and ~3.5 km long in the NNW-SSE direction (Figure 7). Resistivity increases SW from the Pads A and C area towards Mt. Sorik, and peak at 7-20 Ωm near the Sibanggor Julu springs, an extinct or dormant fumarole field (Figure 8). This zone is likely related to a reduced intensity of clay alteration, thought to be associated with more moderate-resistivity, lower-grade alteration, such as mixed clays, above a thicker cap. A <5 Ωm low resistivity zone follows topography up the flanks of the Sorik Marapi volcano, over the summit and terminates on the west and southwest sides of the mountain. This zone is thought to be associated with gravity-driven, condensed supergene fluids flowing down from the summit and altering shallow volcanics, which represent a different source of fluids from the neutral geothermal resource at lower elevations. North of Pads A and D, 1D MT resistivity models resolve a moderate 3-15 Ωm resistivity zone shallowing from 0 masl to >300 masl.

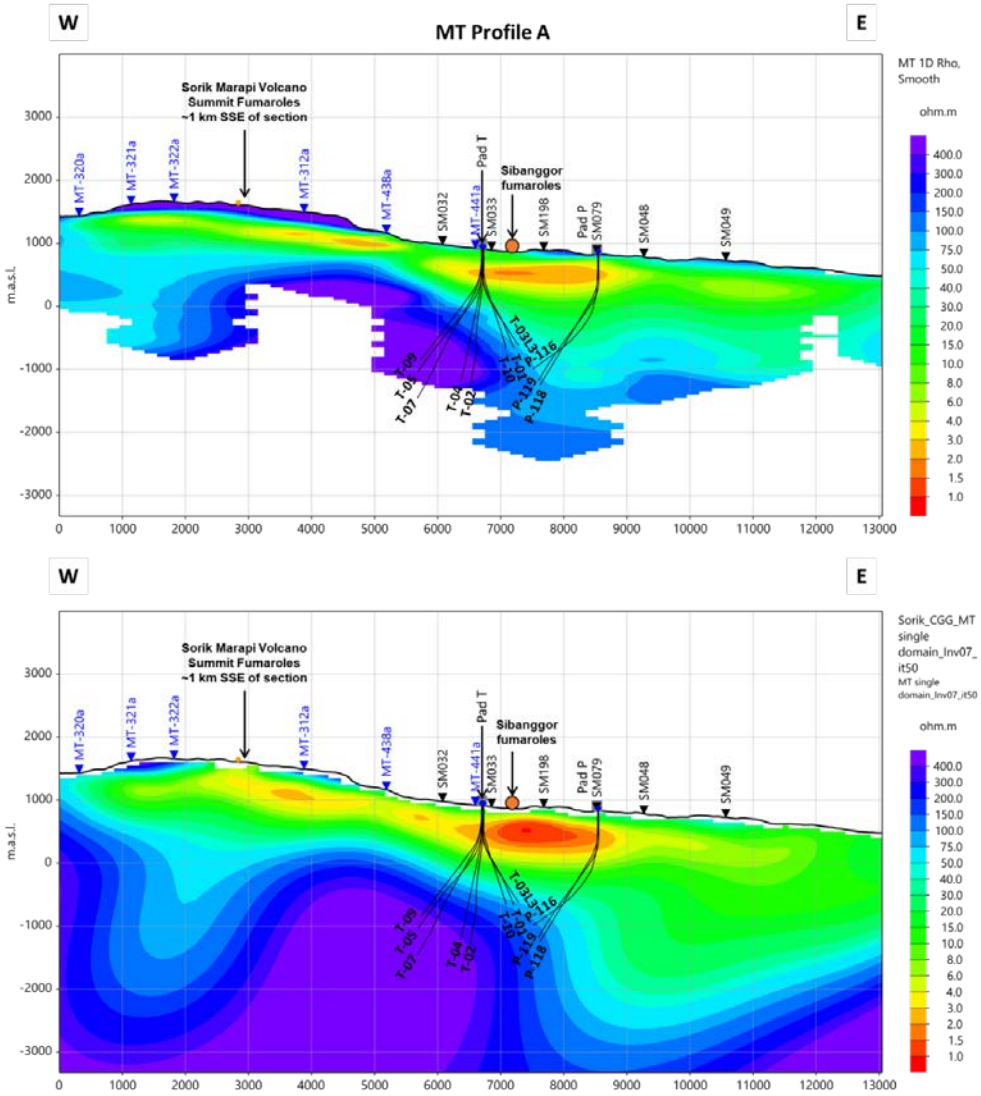

Figure 8: 1D MT resistivity model (upper) and 3D MT resistivity model (lower) along MT Profile A through Pads P and T, the Sibanggor fumaroles, and up the flanks of Sorik Marapi volcano.

Interpretation of the gravity has informed early exploration and constrained the general basin geometry. A gravity low extending from Pad E down to Pads A and T is consistent with deeper, denser basement being down dropped within the western and eastern strands of the SFS (Figure 9). A lower amplitude gravity low continues east of the eastern strand of the SFS and is resolved by thickening QTv and Ts towards the east (Figure 9).

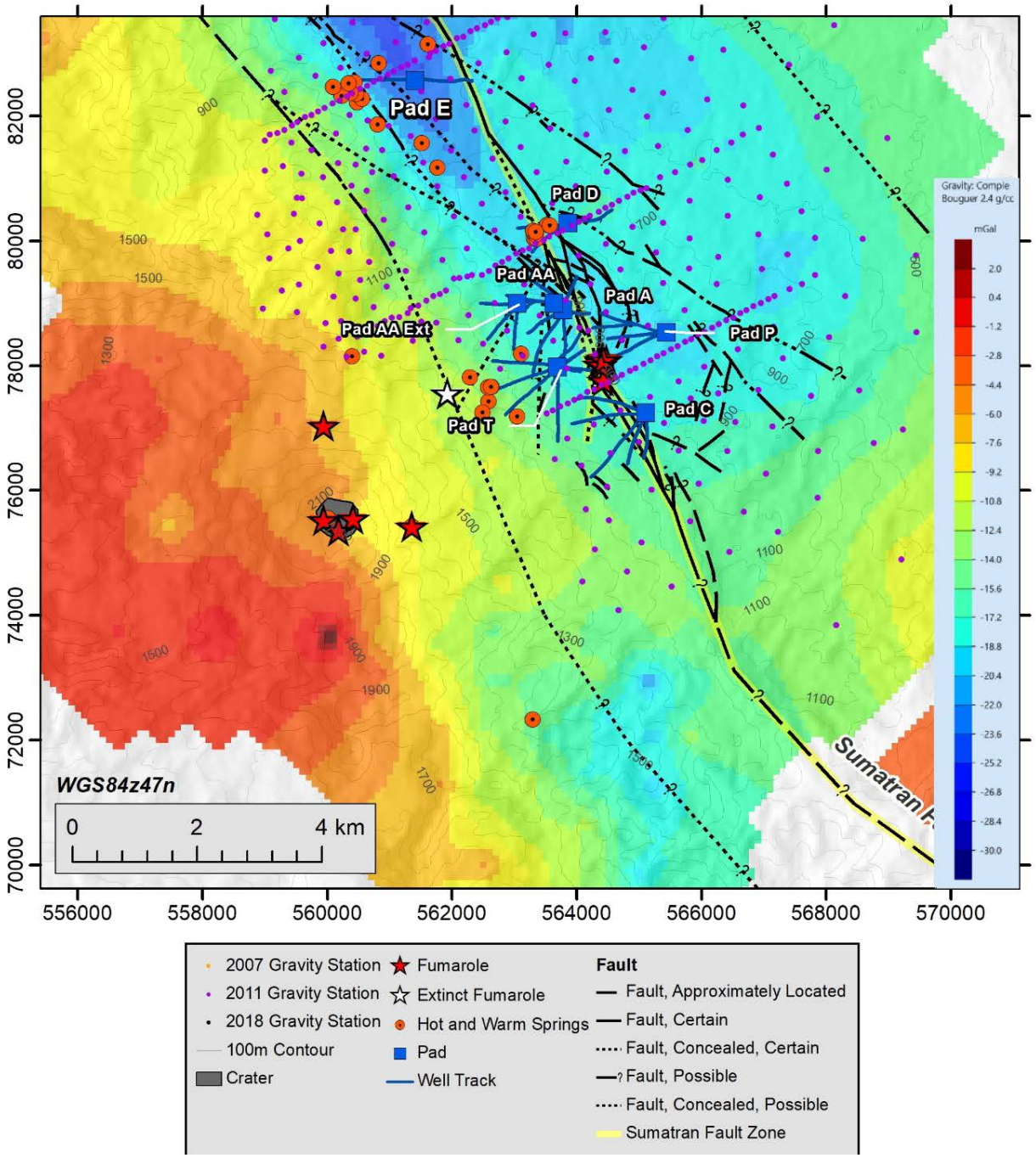

Figure 9: Complete Bouguer Anomaly map evaluated with respect to a density of 2.4 g/cc.

2.4 Well Temperature Data and Reservoir Permeability Patterns

Temperature data obtained in the SMGP wells provide the basis for mapping the location, shape and size of the >240°C geothermal system at Sorik Marapi. Temperatures of select wells on Pads A, C, D, E, and P help define the northern, eastern, and southern boundaries of the >240°C reservoir, while west-directed wells from Pad T point towards the upflow of the system. The Pad A wells show a hot (~250-282°C) zone below 0 masl, while T-09 has a maximum temperature of 323°C below -900 masl. The major and minor feedzones of adjacent wells span from 52 to -1071 masl. In general, the top of reservoir (TOR, based on the elevation of top of isothermal zone) is shallowest in the NE at A-101, A-102, and A-104 and descends to the southwest. Temperatures increase and major feedzones are 500 m to 1200 m lower in elevation from NE to SW, illustrating that the top of the >260°C reservoir drops relatively steeply between A-101/A-104 and T-05, T-09, and T-04.

Based on the revised conceptual geology models and well pressures, Pad E wells lie outside the Sibanggor reservoir. Pad D and P wells have not been flow tested but based on available temperature data and the geology model, these wells also lie outside the main reservoir. Reservoir tracer results obtained to-date using conservative NDS-type tracers indicate that fluids injected into P-116 do return to all Pad A wells. The degree of connection between P-116 and Pad A wells based on tracer data is comparable to production and injection well-pairs on Pads A and C. NDS-type tracers have not yet returned to any Pad A wells from D-108ST during a monitoring period of ~280-days with steady production and injection, and longer term evaluation of chemistry and well pressures will be needed to determine if any of the Pad D wells are in communication with Pad A wells. Based on the geology models and temperature data, the lower parts of A-102 and A-104 appear to exit laterally out of the main part of the reservoir and cross the Sumatra Fault to the NE and E, respectively. At the southern end of the field, wells C-111, C-115, and C-114 were drilled SSE of the >240°C reservoir. Relatively shallow reversals at the base of the capping volcanic rocks in wells C-115 and C-114 support outflow along the Sumatran fault zone to towards the south.

3. Conceptual Model

A commercial geothermal resource at ~245 – 325°C, and with neutral chemistry has been confirmed in a 3 km (N-S) x 1.5 km (E-W) area within the SFS by drilling and testing deep exploration and development wells. Upflow of >300°C is postulated to be focused SW of Pad A, close to the TD of T-09 (Figures 11-12). Cation geothermometry from T-09 is about 300°C, which is up to 25°C lower than the maximum static temperatures in the two hottest wells, T-09 and T-07. The preferred model for this temperature regime is conductive heat input with higher temperatures than the convective heat input, such as would be associated with one or more cooling intrusions >3 km deep. The >240°C outflow is hosted almost entirely in metamorphic and intrusive rocks and rises from SW to NE where it abuts a major strand of the SFS and <240°C outflow continues NW and SE along the west side of this fault strand. The cap over the reservoir is deepest over the upflow and consists of phyllic to propylitic alteration. As the cap rises form SW to NE, the alteration mineralogy of the cap grades from phyllic to mixed clay to argillic at the shallowest parts.

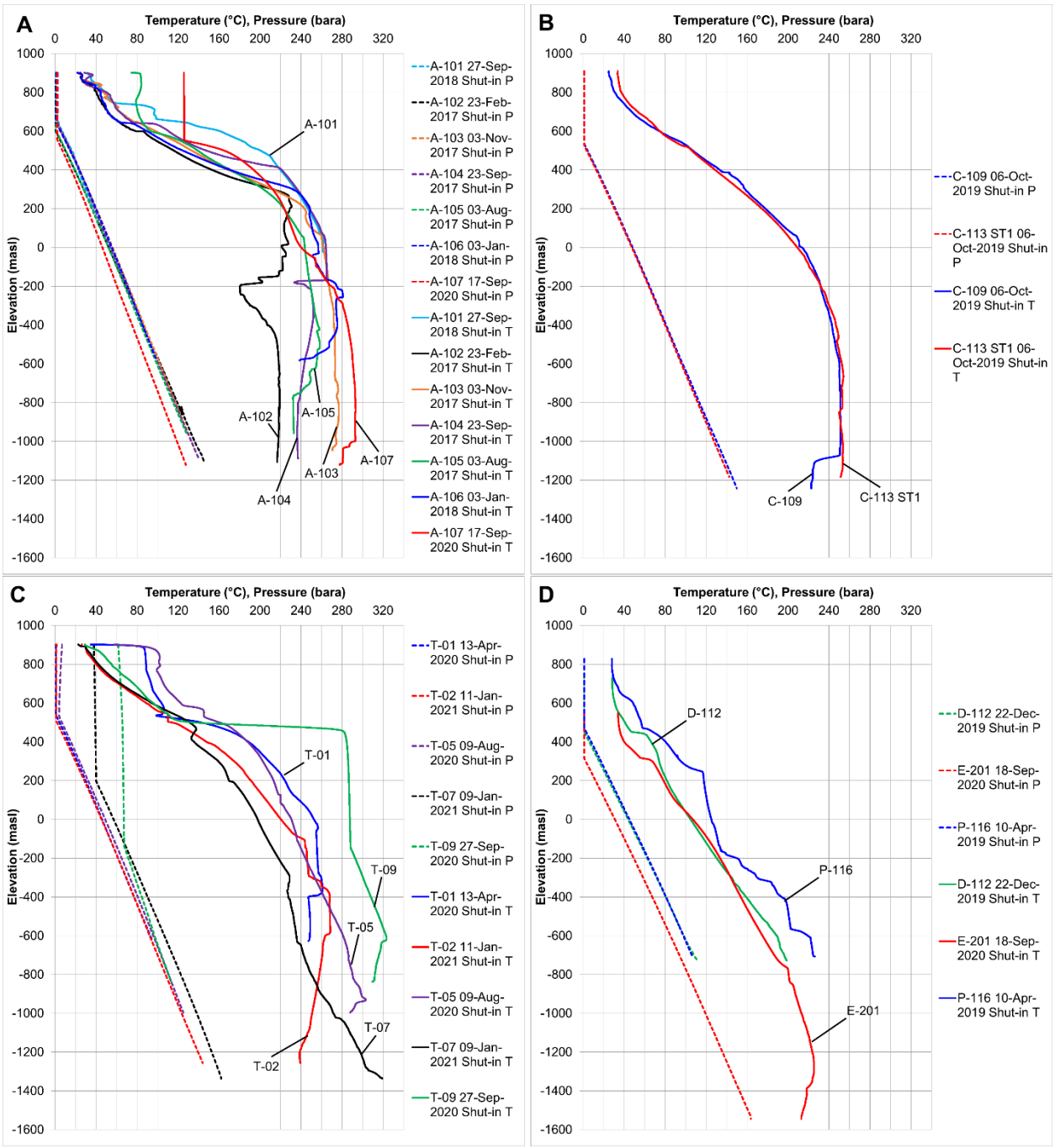

Figure 10. Pressure and temperature plots of the most stable well conditions within the perforated portion of the well for (a) Pad A, (b) Pad C, (c) Pad T, and (d) Pads D, E, and P

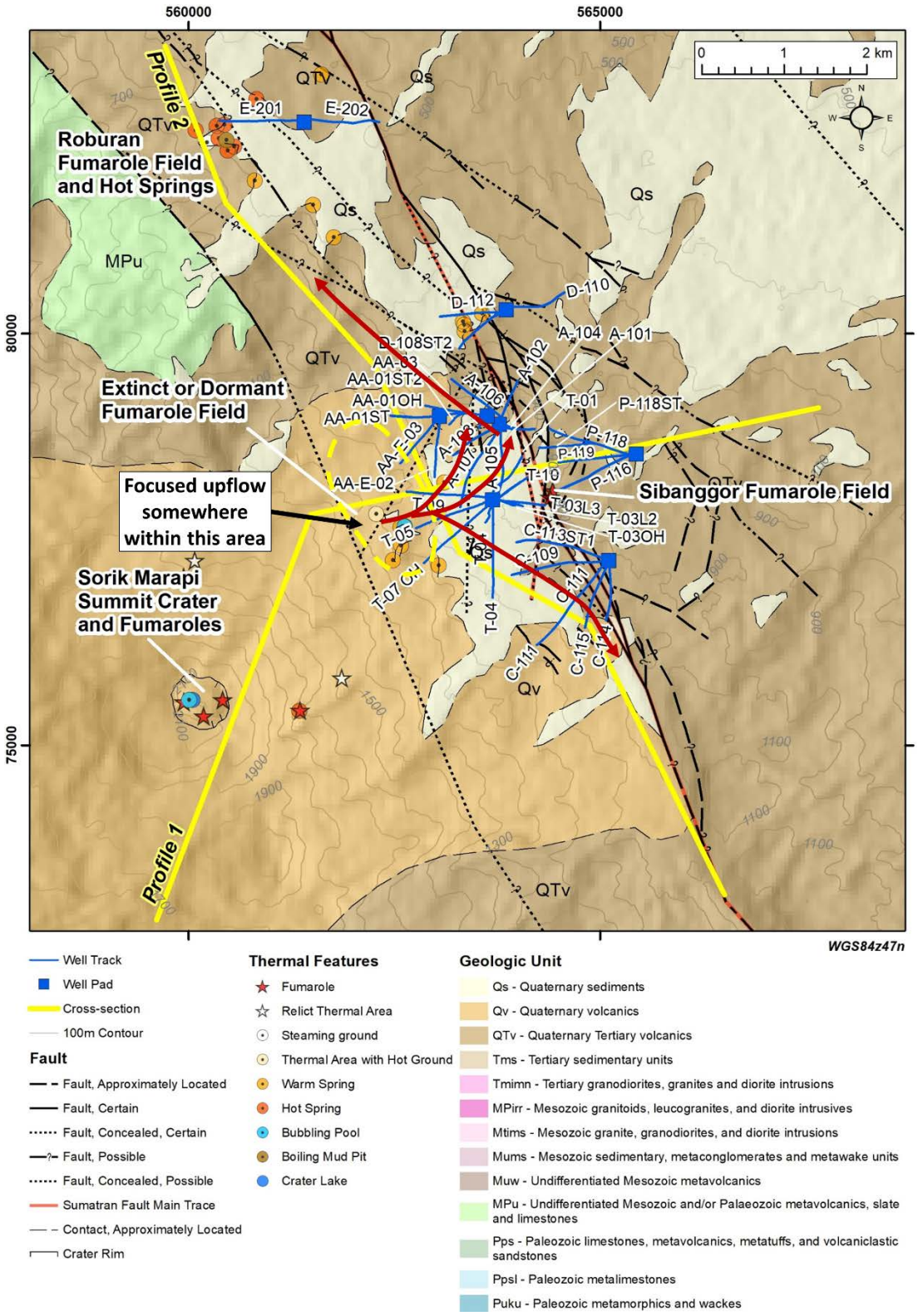

Figure 11. 2021 conceptual model showing the inferred area which contains a focused upflow (yellow dashed line) and easterly outflow within a thick sequence of metasediments and intrusive rocks. The inferred outflow pathways are indicated with red arrows. The location of the concealed western strand of the Sumatran fault and its relationship to the upflow zone is uncertain.

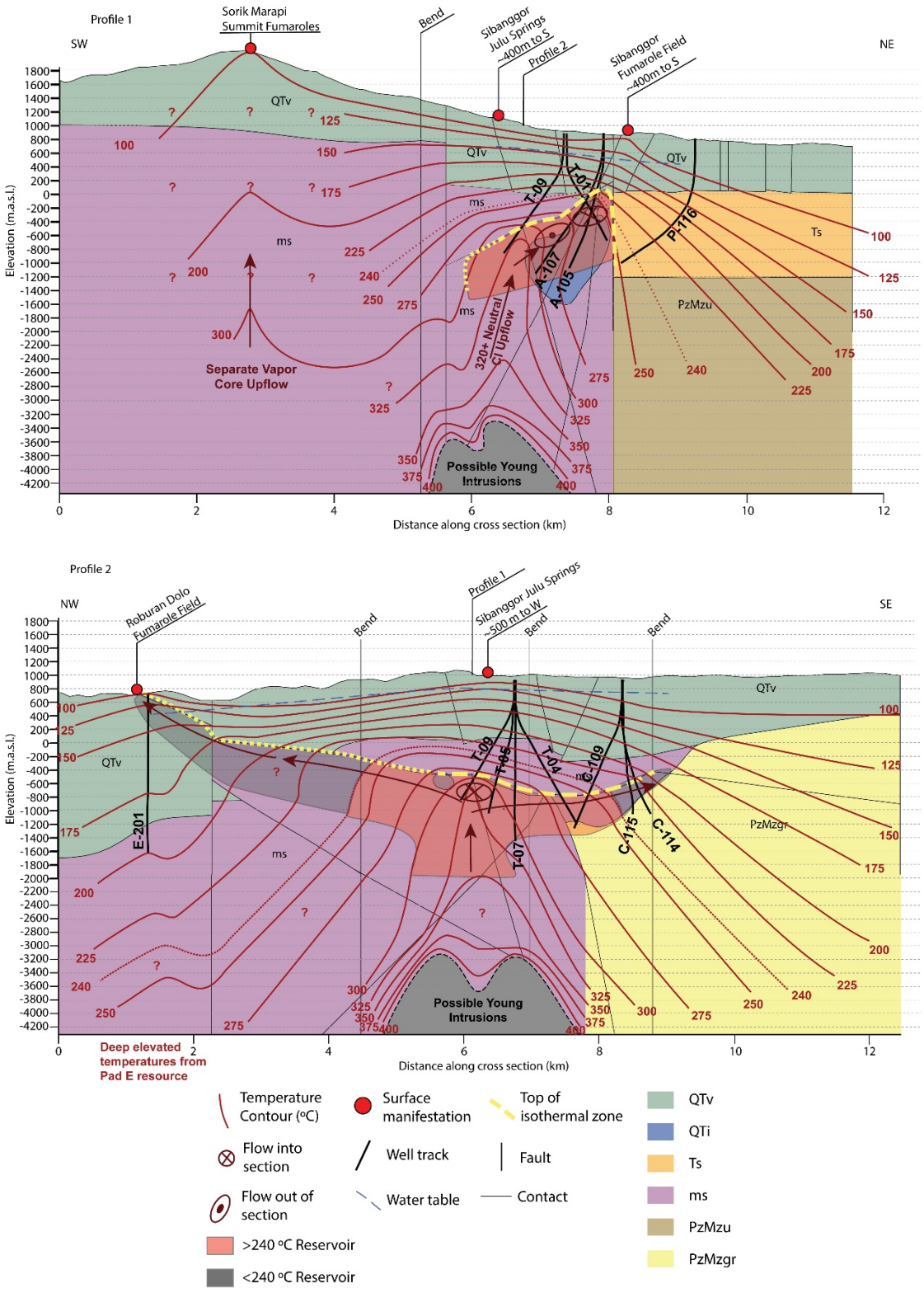

Figure 12. Conceptual model cross sections along Profiles 1 and 2 illustrating isotherms, fluid flow pathways, reservoir boundaries, and the geologic model.

4. Conclusions

Below is a list of key conclusions drawn from this conceptual model update.

- A revised conceptual reservoir model for the field has a deep >300°C upflow near the bottom of well T-09, which feeds the shallower productive reservoir that is tapped by the A, AA, T and northern C pad wells.
- The reservoir is located between two major strands of the Sumatra Fault System. The most active strand bounds the reservoir on the east side, and the upflow may be controlled by a buried strand on the west side.
- Most of the reservoir rock is composed mostly of metasediments (phyllite and quartzite), lesser amounts of Quaternary intrusive rocks, and minor amounts of Tertiary volcanics.
- Although the reservoir mostly hosted in metamorphic and intrusive rocks, the permeability patterns may be controlled by geomechanics associated with pull-apart between two major strands of the Sumatra Fault System.
- The top of isothermal descends from NE to SW across the reservoir with major feed zones located within 50 to 600 vertically below the top of isothermal as defined in static temperature logs. These temperature and feed zone distribution data support that the outflow is somewhat tabular and the top is inclined up and to the NE at about 40°.
- The reservoir cap mineralogy changes from argillic to mixed clay at the apex of the system in the NE to phyllic and eventually propylitic as the top of the reservoir deepens and also gets hotter to the SW.
- Cation geothermometry from T-09 is about 300°C, which is up to 25°C lower than the maximum static temperatures in the two hottest wells, T-09 and T-07. This supports that there is conductive heat input with higher temperatures than the convective heat input.
- There is no evidence that the Sorik Marapi geothermal reservoir has been impacted by magmatic acid vapor cores or supergene acid influx, rather the reservoir is geochemically similar to many other entirely neutral systems developed worldwide.

REFERENCES

Carver, C., and Hidayat, R., 2020, The fluid geochemistry of the Sorik Marapi geothermal reservoir: GRC Transactions, v. 44, 8 p.

CGG Electromagnetics (Italy) Srl., 2019, 3D MT and Gravity Modelling, Sorik Marapi, Sumatra, Indonesia, 88 p.

Hochstein, M.P., and Sudarman, S., 1993, Geothermal resources of Sumatra: Geothermics, v. 22, No. 3, p. 181-200.

Licup, A.C., Sarmiento, Z.F., Omac, X.L., Maneja, F.C., Chandra, VR, Esberto, M.B., Villareal, M.J.Z., Baltasar, A.S.J., Mulyani, S., Sari, P.P., Jhonny, E., and Juandi, D., 2017, Geothermal 3D Subsurface Modeling–A Case Study from Sorik Marapi Field, Indonesia: Proceedings: The 5th Indonesian International Geothermal Convention and Exhibition (IIGCE), 13 p.

Matson, G., Cumming, W., Siagian, H., Hinz, N., Pasikki, R., 2021. Interpretation of Magnetotelluric Resistivity Model of the Sorik Marapi Geothermal Prospect, Sumatra, Indonesia. GRC Transactions, V45.

Rezky, Y., and Hermawan, D., 2015, Geothermal system of Sorik Marapi – Roburan – Sampuraga, North Sumatra, Indonesia: Proceedings World Geothermal Congress 2015, Melbourne, Australia, 19-25 April 2015, 9 p.

Rock, N.M.S., Aldiss, D.T., Aspden, J.A., Clarke, M.C.G., Djunuddin, A., Kartawa, W., Miswar, S.J., Thompson, R. & Whandoyo, R., 1983. The Geology of the Lubuksikaping Quadrangle (0716), Sumatra, Scale 1: 250.000. Geological Survey of Indonesia, Directorate of Mineral Resources, Geological Research and Development Centre, Bandung.

Sarmiento, Z.F., Bjornsson, G., Licup, A.C., Esberto, M.B., Indra, T., Balstasar, A.S.J, Maneja, F.C., Omac, X.L., Villareal, M.J.Z., and Chandra, V., 2017, Update on the exploration and development drilling at the Sorik Marapi Geothermal Field, North Sumatra, Indonesia: Proceedings: The 5th Indonesian International Geothermal Convention and Exhibition (IIGCE), 8 p.

SKM, 2011, Sorik Marapi Preliminary Resource Assessment Report: proprietary report, 369 p.